

OBJECT-AWARE LIFTING FOR 3D SCENE SEGMENTATION IN GAUSSIAN SPLATTING

Anonymous authors

Paper under double-blind review

In this supplementary material, we provide more implementation details (Sec. A), more quantitative and qualitative comparisons (Sec. B), and more detailed analysis (Sec. C) about our proposed method.

A IMPLEMENTATIONS DETAILS

We implement our method based on the 3D Gaussian Splatting (3D-GS) Kerbl et al. (2023) representation. Specifically, we set the dimension of the Gaussian-level feature as 16 to maintain a fair comparison with previous baselines (*e.g.*, Gaussian Grouping (Ye et al., 2023) and OmniSeg3D-GS (Ying et al., 2024)). For the learning of original properties in 3D Gaussian points, we use the same learning rate and same density control as the in the original work (Kerbl et al., 2023). For the Gaussian-level feature, we utilize the Adam optimizer with a learning rate of 0.0025. For the object-level code, we employ the Adam optimizer with a learning rate of 0.0005. We jointly train all parameters for 30,000 iterations on each dataset covered in this work, using a single NVIDIA RTX 3090.

B MORE QUANTITATIVE AND QUALITATIVE COMPARISONS

Quantitative comparisons with OmniSeg3D-GS. Since OmniSeg3D-GS (Ying et al., 2024) only learns feature embeddings, we equip OmniSeg3D-GS with HDBSCAN clustering algorithm (McInnes et al., 2017) to produce the final segmentation results. We report the performance under the optimal best-found hyper-parameter (*i.e.*, minimal cluster size) for HDBSCAN, following the same strategy used in Contrastive Lift (Bhalgat et al., 2023). Specifically, we utilize the training views to search for the best hyper-parameter for each scene, setting the search range from 10 to 200, as suggested in “Tuning Clustering Hyperparameter” (Bhalgat et al., 2023). As shown in Fig. 1, while the exhaustive search can improve performance, it is still behind our method, which achieves consistent results without the need for hyperparameter tuning.

Qualitative comparisons. In addition to the visual results presented in the main paper, we provide more qualitative comparisons in Fig. 2, Fig. 3 and Fig. 4. These visual results further demonstrate that our method delivers more accurate and consistent segmentation across various views, while also minimizing artifacts.

C MORE ANALYSIS OF PROPOSED COMPONENTS

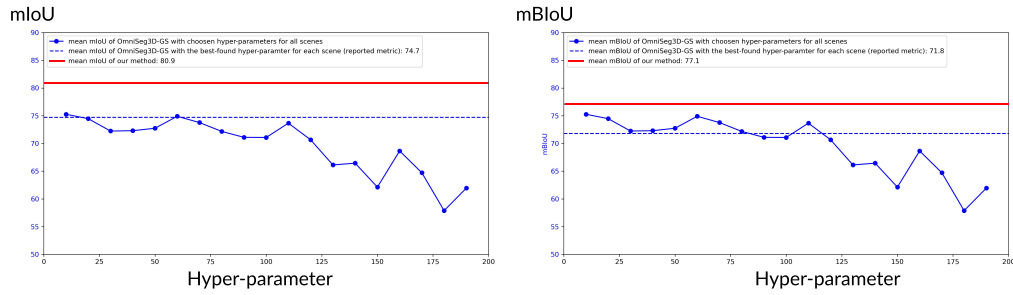
Table 1: Effectiveness analysis of the proposed area-aware ID mapping method. We compare the segmentation results of pseudo-labels generated by our area-aware ID mapping and the approach proposed in Panoptic Lifting (Siddiqui et al., 2023).

| ID matching strategy | mIoU(%) | F-score(%) |
|--------------------------------|---------|------------|
| Siddiqui et al. (2023) | 30.3 | 30.4 |
| Proposed area-aware ID mapping | 31.7 | 33.5 |

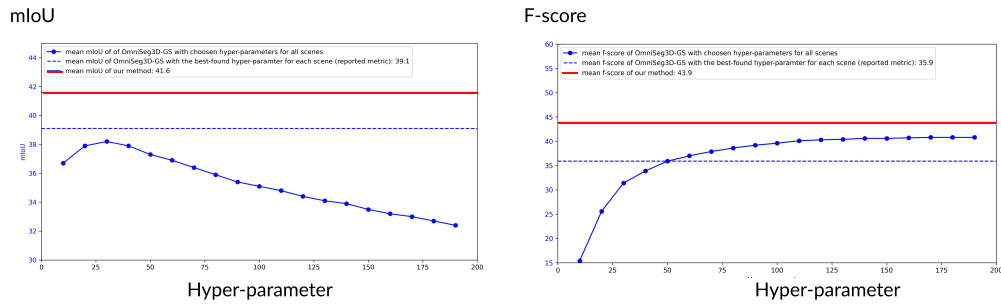
Area-aware ID mapping. To further verify the effectiveness of our area-aware ID mapping, we present additional quantitative comparisons between the generated pseudo-labels by our area-aware

054
055
056
057
058
059
060
061
062
063
064
065
066
067
068
069
070
071
072
073
074
075
076
077
078
079
080
081
082
083
084
085
086
087
088
089
090
091
092
093
094
095
096
097
098
099
100
101
102
103
104
105
106
107

(a) LERF-Masked dataset



(b) Replica dataset



(c) Messy Rooms dataset

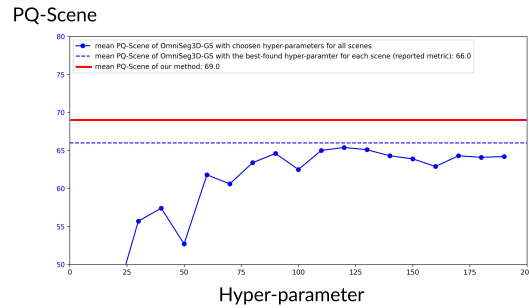


Figure 1: The detailed comparison between our method and OmniSeg3D-GS methods on the LERF-Mask dataset (Ye et al., 2023), Replica dataset (Straub et al., 2019) and the Messy Rooms dataset (Bhalgat et al., 2023) dataset. For LERF and Replica datasets, we utilize the mIoU metric to search the best hyper-parameter for each scene. For the Messy Rooms dataset, we utilize the PQ-Score to select the best hyper-parameter for each scene. Note that our method is denoted by the red color, and OmniSeg3D-GS is denoted by the blue color.

Table 2: Quantitative comparisons of using different thresholds τ values in the noisy label filtering module.

| τ | 0.75 | 0.80 (default) | 0.85 |
|------------|------|----------------|------|
| mIoU(%) | 40.0 | 41.6 | 40.4 |
| F-score(%) | 43.0 | 43.9 | 43.7 |

ID mapping method and the method proposed in Panoptic Lifting (Siddiqui et al., 2023). The results shown in Tab. 1 verify that the pseudo-labels generated by our area-aware ID mapping are more accurate and consistent.

Sensitivity to different per-defined values in noisy label filtering. We investigate the impact of varying the predefined threshold used to filter noisy labels in the noisy label filtering module. In

Table 3: Ablation study on the effectiveness of our gradient-blocking design.

| Method | mIoU(%) | F-score (%) |
|---|---------|-------------|
| Full model | 41.6 | 43.9 |
| Full model w/o gradient-blocking design | 39.7 | 39.8 |

our main experiments, we set a predefined threshold of $\tau = 0.8$ to filter noisy segmentations in the noisy label filtering module. To investigate the impact of this threshold, we conduct additional experiments using two different values ($\tau = 0.75$ and 0.85). As shown in Tab. 2, the results remain rather stable despite moderate changes in the threshold τ .

Gradient-blocking. In practice, we block the gradient derived from the association constraints from propagating to the Gaussian-level features. This gradient-blocking design ensures that the Gaussian-level features are exclusively optimized through the contrastive loss. The ablation study in Tab. 3 demonstrates that this design improves optimization stability.

162
163
164
165
166
167
168
169
170
171
172
173
174
175
176
177
178
179
180
181
182
183
184
185
186
187
188
189
190
191
192
193
194
195
196
197
198
199
200
201
202
203
204
205
206
207
208
209
210
211
212
213
214
215

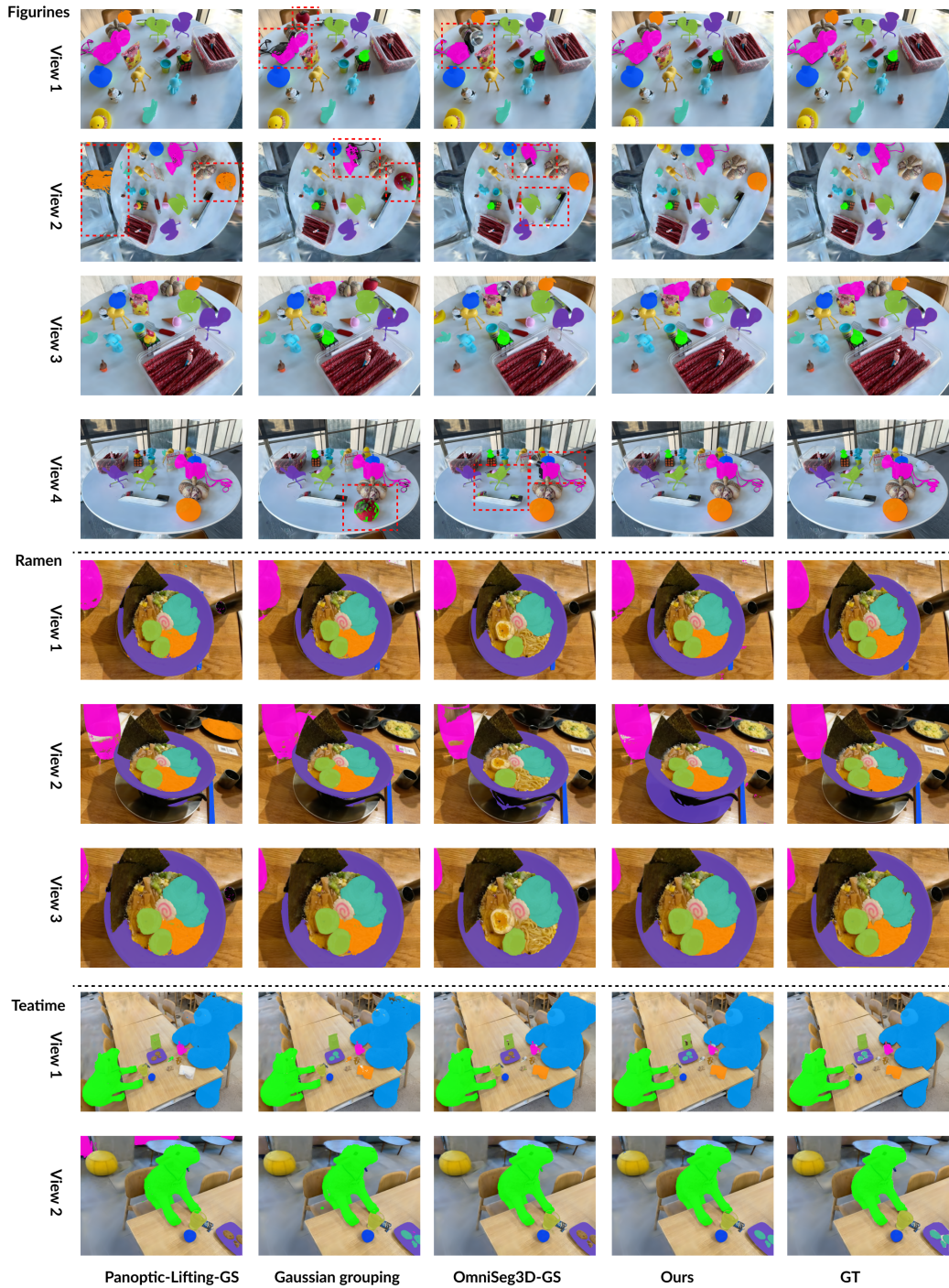


Figure 2: Visual comparisons between our method and previous methods on the LERF-Masked dataset (Ye et al., 2023).

216
217
218
219
220
221
222
223
224
225
226
227
228
229
230
231
232
233
234
235
236
237
238
239
240
241
242
243
244
245
246
247
248
249
250
251
252
253
254
255
256
257
258
259
260
261
262
263
264
265
266
267
268
269

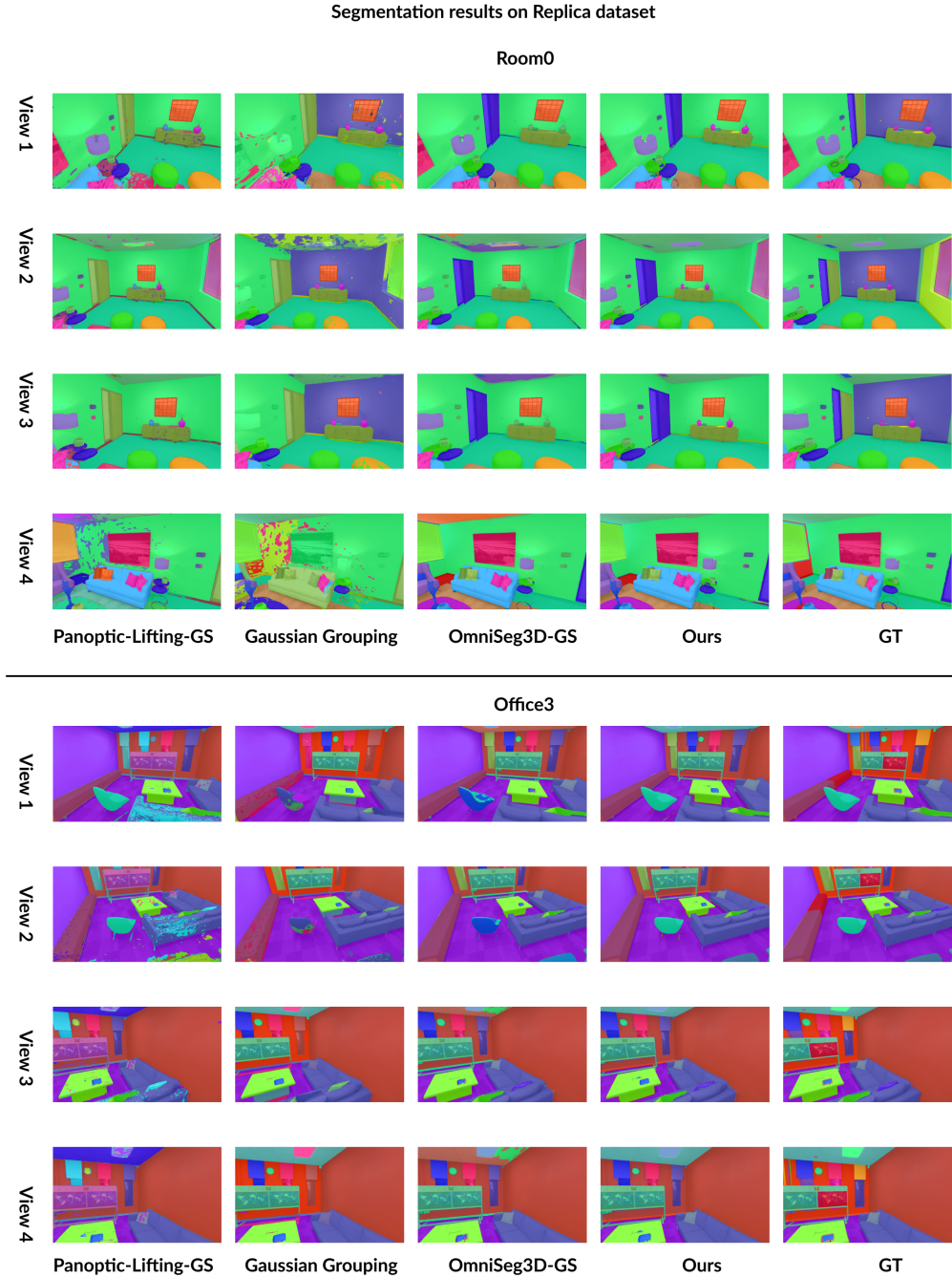


Figure 3: Visual comparisons between our method and previous methods on the Replica dataset (Straub et al., 2019).

270
 271
 272
 273
 274
 275
 276
 277
 278
 279
 280
 281
 282
 283
 284
 285
 286
 287
 288
 289
 290
 291
 292
 293
 294
 295
 296
 297
 298
 299
 300
 301
 302
 303
 304
 305
 306
 307
 308
 309
 310
 311
 312
 313
 314
 315
 316
 317
 318
 319
 320
 321
 322
 323

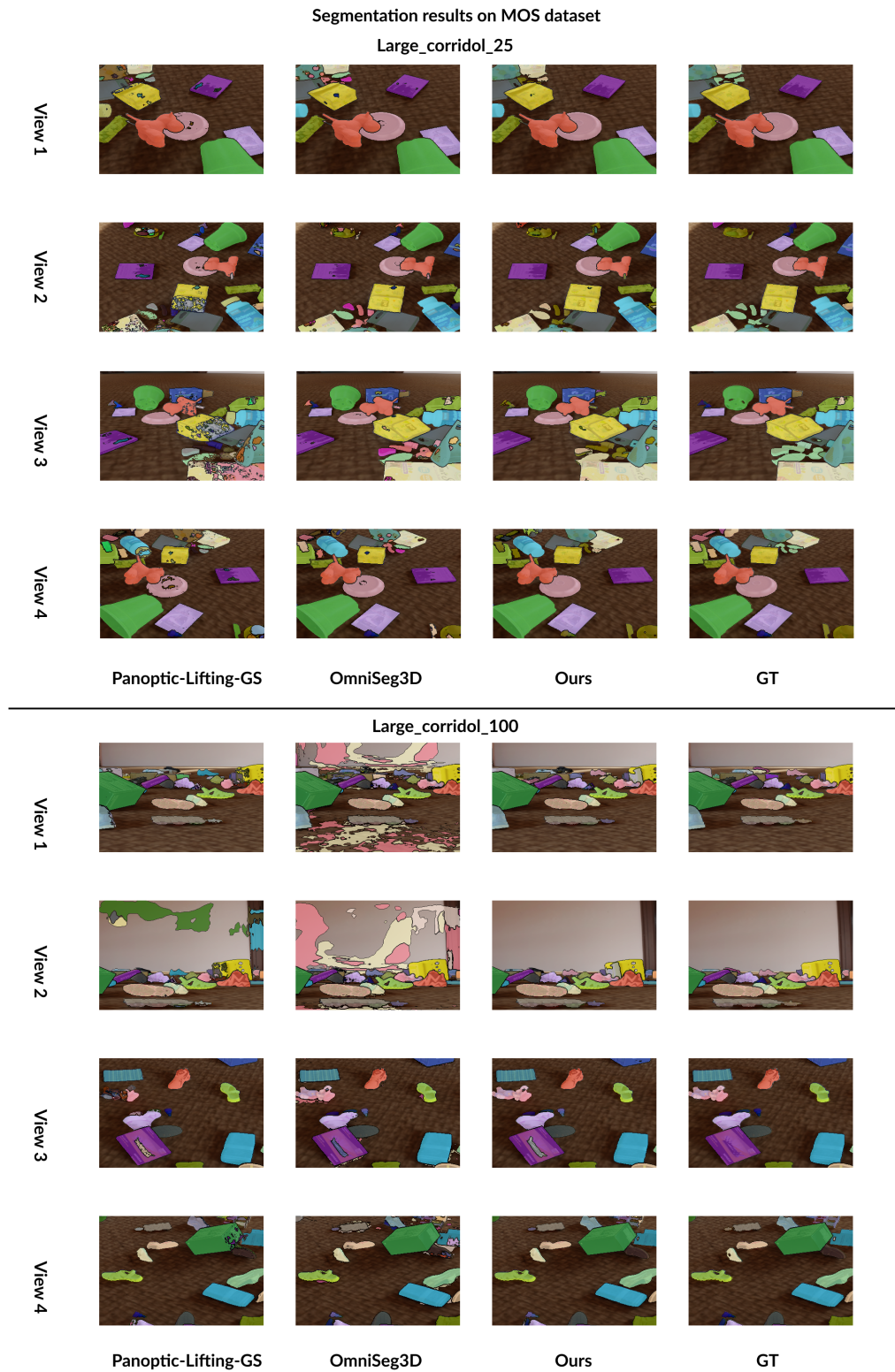


Figure 4: Visual comparisons between our method and previous methods on the Messy Rooms dataset (Straub et al., 2019).

324
325
326
327
328
329
330
331
332
333
334
335
336
337
338
339
340
341
342
343
344
345
346
347
348
349
350
351
352
353
354
355
356
357
358
359
360
361
362
363
364
365
366
367
368
369
370
371
372
373
374
375
376
377

REFERENCES

- Yash Bhalgat, Iro Laina, João F Henriques, Andrew Zisserman, and Andrea Vedaldi. Contrastive Lift: 3D object instance segmentation by slow-fast contrastive fusion. *arXiv preprint arXiv:2306.04633*, 2023.
- Bernhard Kerbl, Georgios Kopanas, Thomas Leimkühler, and George Drettakis. 3D gaussian splatting for real-time radiance field rendering. *ACM Transactions on Graphics*, 42(4), 2023.
- Leland McInnes, John Healy, and Steve Astels. hdbscan: Hierarchical density based clustering. *J. Open Source Softw.*, 2(11):205, 2017.
- Yawar Siddiqui, Lorenzo Porzi, Samuel Rota Bulò, Norman Müller, Matthias Nießner, Angela Dai, and Peter Kotschieder. Panoptic lifting for 3D scene understanding with neural fields. In *Proceedings of the IEEE/CVF Conference on Computer Vision and Pattern Recognition*, pp. 9043–9052, 2023.
- Julian Straub, Thomas Whelan, Lingni Ma, Yufan Chen, Erik Wijmans, Simon Green, Jakob J Engel, Raul Mur-Artal, Carl Ren, Shobhit Verma, et al. The replica dataset: A digital replica of indoor spaces. *arXiv preprint arXiv:1906.05797*, 2019.
- Mingqiao Ye, Martin Danelljan, Fisher Yu, and Lei Ke. Gaussian grouping: Segment and edit anything in 3D scenes. *arXiv preprint arXiv:2312.00732*, 2023.
- Haiyang Ying, Yixuan Yin, Jinzhi Zhang, Fan Wang, Tao Yu, Ruqi Huang, and Lu Fang. Omnise3d: Omniversal 3d segmentation via hierarchical contrastive learning. In *Proceedings of the IEEE/CVF Conference on Computer Vision and Pattern Recognition*, pp. 20612–20622, 2024.